



Contents lists available at ScienceDirect

Journal of Molecular Liquids

journal homepage: www.elsevier.com/locate/molliq

A general approach based on morphological thermodynamics for a fluid confined in various porous media

C.Z. Qiao^{a,1}, H.R. Jiang^{a,b,1}, S.L. Zhao^{a,c,*}, W. Dong^{b,*}

^a State Key Laboratory of Chemical Engineering and School of Chemical Engineering, East China University of Science and Technology, Shanghai 200237, China

^b Laboratoire de Chimie, Ecole Normale Supérieure de Lyon, CNRS, UMR 5182, 46, Allée d'Italie, 69364 Lyon Cedex 07, France

^c Guangxi Key Laboratory of Petrochemical Resource Processing and Process Intensification Technology and School of Chemistry and Chemical Engineering, Guangxi University, Nanning 530004, China

ABSTRACT

We propose a general approach based on morphological thermodynamics for determining adsorption isotherms, i.e., the chemical potential of a confined fluid as a function of its density. The validity of this approach and its versatility are established by its remarkable accuracy compared to Monte-Carlo simulation results and its capability of accounting for a quite large variety of porous media, ranging from a simple slit pore to a random sponge matrix. It is also revealed that the contribution of the curvature terms to the chemical potential of the confined fluid is negligibly small when the interface curvature is not too large. This finding is of a particular importance for simplifying the treatment of experimental results of adsorption isotherms since no experimental technique is currently available for determining the curvatures of the pore surface inside a porous material.

1. Introduction

Porous materials are widely used in various domains, e.g., in chemical industry for molecular sieves and supported catalysts, in new clean energy technology for storing hydrogen, in some new therapy for long-lasting delivery of medicines by encapsulation. It is now well recognized that confinement can modify drastically some properties of adsorbed fluids. Accompanying the advent of many high-performance functionalized nanoporous materials, a large number of experimental and theoretical investigations have been made during the last decades. Nevertheless, a unifying picture highlighting the behavior of confined fluids emerges quite slowly due to the large diversity of structure and morphology for various porous materials. One salient characteristic of fluids confined in porous media is the large interface between fluid and pore wall, which has usually a complex morphology. Although one expects intuitively an important surface contribution to the thermodynamic potentials of such systems, it is not obvious whether it is still possible to define a meaningful surface tension when the characteristic pore size is of the order of a few molecular diameters of the confined fluid. Even if an approach based on thermodynamics is possible, one still needs to know which are the most relevant variables for characterizing the complex interface landscape of fluids adsorbed in porous media. The theoretical study of fluids confined

in porous media is still carried out essentially in a case-by-case way. The morphological thermodynamics proposed and advocated by K. Mecke, R. Roth and co-workers [1–8] provides a framework for a general thermodynamic description of complex interfacial systems. Starting from Hadwiger's theorem in integral geometry, morphological thermodynamics postulates that four geometrical measures are enough to characterize the thermodynamic potential of a complex interfacial system, i.e., volume, surface area, integrated mean curvature and integrated Gauss curvature [1]. Moreover, Mecke et al assume that the thermodynamic variables conjugated to these geometrical measures, i.e. pressure, surface tension, as well as two surface bending rigidities, can be determined for a simple system then be used to describe systems with more complex morphology [1–3]. Although morphological thermodynamics gives promising results for some systems [1–8], the validity of one of its fundamental postulates has been questioned. Theoretical and simulation investigations have provided evidence for the existence of non-Hadwiger terms, i.e., high-order curvature contributions to surface tension, which are not taken into account in the morphological thermodynamics [9–12]. Moreover, these investigations have shown that the first non-Hadwiger term gives a contribution much smaller than the Hadwiger terms, at least one order of magnitude smaller [9]. Hence, morphological thermodynamics can allow for formulating useful approximations in practice even when Hadwiger

* Corresponding authors at: State Key Laboratory of Chemical Engineering and School of Chemical Engineering, East China University of Science and Technology, Shanghai 200237, China.

E-mail addresses: szhao@ecust.edu.cn (S.L. Zhao), wei.dong@ens-lyon.fr (W. Dong).

¹ Authors contribute equally to this work.

<https://doi.org/10.1016/j.molliq.2023.123345>

Received 31 May 2023; Received in revised form 2 October 2023; Accepted 12 October 2023

Available online 13 October 2023

0167-7322/© 2023 Elsevier B.V. All rights reserved.

theorem does not hold rigorously. Fluids adsorbed in porous materials with a complex morphology of pore space provide an interesting ground for further testing the applicability of morphological thermodynamics. This constitutes the main objective of the present work. Some of us (SLZ and WD) have collaborated during a long time with Myroslav Holovko in the study of fluids confined in porous media [13–17]. It is our great pleasure to dedicate the present article to this special issue for the eightieth anniversary of Professor Holovko.

Our presentation is organized as follows. A brief introduction of morphological thermodynamics and a general equation of state for a fluid confined in various porous media will be presented in the next section. The accuracy of the general equation of state in different confining media will be assessed in Section 3. Some conclusions will be presented in the last section.

2. Theory

2.1. A brief recall of morphological thermodynamics

The morphological thermodynamics proposed by Mecke, Roth and coworkers is based on the fundamental assumption that the grand potential of a complex interfacial system is a linear combination of four morphological measures, i.e., the system's volume, V , the interface area, A , the integrated mean curvature, C_M , and the integrated Gauss curvatures, C_G . From this assumption, one has immediately the following expression for the grand potential,

$$\Omega = -p^{\text{bulk}}(T, \mu)V + \gamma_0(T, \mu)A + \gamma_{-1}(T, \mu)C_M + \gamma_{-2}(T, \mu)C_G \quad (1)$$

where T is temperature, μ the chemical potential. The coefficients of the morphological measures are respectively the pressure of the corresponding bulk system, p^{bulk} , the surface tension on a flat surface, γ_0 , and the bending rigidities, γ_{-1} and γ_{-2} related to the integrated mean and Gauss curvatures. Before applying it to study fluids confined in porous media, it is useful to clarify further some implications of the morphological thermodynamics given in Eq. (1). First, it is to note that the morphological measures are completely decoupled with the properties of the fluid, i.e., the four morphological measures being independent of the fluid state, i.e., T and μ . Such decoupling allows for separating the study of a complex interfacial system into two simpler tasks, one for determining the morphological measures in the absence of the fluid and the other for determining the coefficients, γ_0 , γ_{-1} and γ_{-2} , from a simpler system, e.g., the considered fluid near a spherical surface. On the other hand, the independence of the morphological measures on the fluid state does not hold for fluid adsorption in very flexible porous materials since the adsorption can induce large deformation of the materials and modify significantly their morphology. So, the morphological thermodynamics as presented above cannot be applied for the fluid adsorption in flexible porous materials. We can also rewrite Eq. (1) as,

$$\Omega = \Omega^{\text{bulk}} + \hat{\gamma}A \quad (2)$$

where

$$\hat{\gamma} = \gamma_0(T, \mu) + \gamma_{-1}(T, \mu) \frac{C_M}{A} + \gamma_{-2}(T, \mu) \frac{C_G}{A} \quad (3)$$

Recently, one of us has shown that it is necessary to introduce the concepts of differential and integral surface tensions for strongly confined fluids, i.e., pore size being sufficiently small so that γ_0 , γ_{-1} and γ_{-2} in Eq. (3) can also depend on the pore size in addition of T and μ [18,19]. Although $\hat{\gamma}$ defined from Eq. (2) is an integral surface tension, the assumption that γ_0 , γ_{-1} and γ_{-2} are only functions of temperature and chemical potential is too restrictive to account for more complex situations. Therefore, we can anticipate that the morphological thermodynamics can become less and less accurate when confinement becomes stronger and stronger.

2.2. Adsorption isotherms based on morphological thermodynamics

The morphological thermodynamics extends Gibbs surface thermodynamics by proposing a concrete recipe to account for the curvature contributions in the grand potential. It is straightforward to show that the surface tension given in Eq. (2) satisfies Gibbs adsorption equation, i.e.,

$$\left(\frac{\partial \hat{\gamma}}{\partial \mu}\right)_T = \frac{1}{A} \left[\left(\frac{\partial \Omega}{\partial \mu}\right)_T - \left(\frac{\partial \Omega^{\text{bulk}}}{\partial \mu}\right)_T \right] = \frac{N_1 - N^b}{A} = -\Gamma \quad (4)$$

where Γ is defined as adsorption, N_1 and N^b are respectively the particle number of the confined fluid and that of the corresponding bulk fluid in the same volume with the same temperature and chemical potential. This equation provides a relation between the density of the confined fluid, $\rho_1 = N_1 V^{-1}$, and that of the corresponding bulk fluid, $\rho^b = N^b V^{-1}$,

$$\rho^b = \rho_1 + \left(\frac{\partial \hat{\gamma}}{\partial \mu}\right)_T \frac{A}{V} \quad (5)$$

Now, from the equation of state of the bulk fluid and the relation given by Eq. (5), we obtain immediately the following equation of state for the confined fluid,

$$\mu(\rho_1) = \mu^{\text{bulk}} \left[\rho_1 + \left(\frac{\partial \hat{\gamma}}{\partial \mu}\right)_T \frac{A}{V} \right] \quad (6)$$

3. Results and discussion

The theoretical framework presented in the last section is a quite general one which can be applied for studying a large variety of confined fluids. We illustrate this by considering some benchmark model systems.

3.1. A hard sphere fluid confined in a slit pore with hard walls

We consider first a hard sphere (HS) fluid confined in a slit pore formed with two parallel hard walls. A schematic presentation of such a system is given in Fig. 1. The morphological thermodynamic approach described in Section 2.2 is based on two prerequisites: i) an equation of state for the bulk fluid; ii) the surface tension for the considered interface. For a HS fluid confined in a slit pore with two hard walls, scaled particle theory (SPT) [20–22] provides both the equation of state of the bulk fluid and the surface tension of a HS fluid near a flat hard wall.

The SPT equation of state for a bulk HS fluid is given by,

$$\beta\mu^{\text{SPT}} = \ln(\Lambda^3 \rho^b) - \ln(1 - \eta^b) + \frac{7\eta^b}{1 - \eta^b} + \frac{15}{2} \left(\frac{\eta^b}{1 - \eta^b}\right)^2 + 3 \left(\frac{\eta^b}{1 - \eta^b}\right)^3 \quad (7)$$

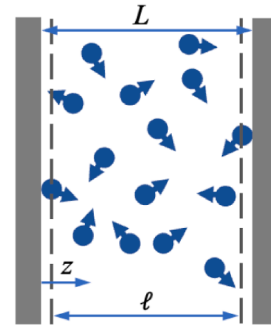


Fig. 1. Schematic presentation of a fluid of hard spheres (blue spheres) confined in a slit pore with two walls (grey) separated by a distance of L (surface normal along the z -direction). The dashed lines mark the closest accessible planes for the hard-sphere centers, $l = L - \sigma$ being the accessible width (σ : fluid hard sphere diameter).

where Λ is the thermal wavelength, $\beta = (k_B T)^{-1}$ (k_B : Boltzmann constant), $\eta^b = \pi\sigma^3\rho^b 6^{-1}$ is the packing fraction of the bulk fluid. The surface tension for a fluid-wall interface and the adsorption depend on the choice of Gibbs dividing surface. For the present work, we choose the wall surfaces located at $z = \pm L/2$ as the dividing surfaces (see Fig. 1). For this choice, the SPT gives the following result for the surface tension,

$$\pi\sigma^2\beta\gamma_0^{\text{SPT}} = \frac{3\eta^b}{1-\eta^b} + \frac{9}{2} \left(\frac{\eta^b}{1-\eta^b} \right)^2 \quad (8)$$

From the Gibbs adsorption equation, i.e., Eq. (4), and the results given in Eqs. (7) and (8), we obtain straightforwardly the adsorption on one pore wall,

$$\pi\sigma^2\Gamma_0^{\text{SPT}} = -\pi\sigma^2 \left(\frac{\partial\gamma_0^{\text{SPT}}}{\partial\mu^{\text{SPT}}} \right)_T = -\pi\sigma^2 \frac{(\partial\gamma_0^{\text{SPT}}/\partial\eta^b)_T}{(\partial\mu^{\text{SPT}}/\partial\eta^b)_T} = -\frac{3\eta^b(1-\eta^b)}{1+2\eta^b} \quad (9)$$

Since the slit pore is composed of two hard walls, we have the following relation between the packing fraction of the confined fluid, $\eta_1 = \pi\sigma^3\rho_1 6^{-1}$, and that of the bulk one,

$$\eta_1 = \eta^b + \frac{2\pi\sigma^2\Gamma_0^{\text{SPT}}}{6L^*} = \eta^b - \frac{\eta^b(1-\eta^b)}{L^*(1+2\eta^b)} \quad (10)$$

where $L^* = L\sigma^{-1}$ is the pore width measured with the HS diameter. Since Eq. (10) is a second order polynomial, we obtain the following explicit expression of η^b in terms of η_1 ,

$$\eta^b = \frac{1-L^*+2L^*\eta_1 + \sqrt{(1-L^*+2L^*\eta_1)^2 + 4L^*(1+2L^*)\eta_1}}{2(1+2L^*)} \quad (11)$$

Now, the adsorption isotherm for a HS fluid confined in a slit pore is given by,

$$\beta\mu(\eta_1) = \beta\mu^{\text{bulk}}(\eta^b) \quad (12)$$

The right-hand-side of Eq. (12) is given by substituting Eq. (11) into Eq. (7). Eq. (10) shows clearly that with the increase of L^* , the difference between η_1 and η^b becomes smaller and smaller and $\lim_{L^* \rightarrow \infty} \eta_1 = \eta^b$, one

recovers the bulk result from Eq. (12) for $L^* \rightarrow \infty$ as one can expect. For point particle, i.e. $\sigma = 0$, Eqs. (7) and (12) gives the same exact result for the confined and the bulk ideal gas as we expect.

In Fig. 2, some results given by Eq. (12) are presented for a few pore widths and compared to the results of Monte-Carlo (MC) simulations. Since the adsorption for this system is negative, the adsorption isotherms of the confined fluid are always above the isotherm of the bulk fluid. As the surface contribution decreases when the pore width becomes larger, the isotherm of the confined fluid approaches more and more the isotherm of the bulk fluid. The agreement between the results of morphological thermodynamics and those of the MC simulations is very good for $L^* \geq 3.5$.

Fig. 3 shows the results for some narrower pores, $L^* \leq 3.0$. Up to the moderate fluid density, i.e., $\rho_1\sigma^3 \leq 0.6$, morphological thermodynamics gives accurate results. For higher densities, the results of morphological thermodynamics deviate more and more from those of the MC simulations. For very narrow pores, a disjoining pressure [23,24] arises in the confined fluid. One of us (WD) has shown that due to the contribution of the disjoining pressure, the surface tension for very narrow pores is no longer equal to that for the fluid near one single wall [18]. However, the contribution of the disjoining pressure is not accounted for by the morphological thermodynamics. We believe this is the main reason for the failure of morphological thermodynamics in describing accurately the strongly confined fluids at high densities in very narrow slit pores.

Slit pore is a model extensively used for studying confined fluids. Many simulations have been carried out for fluids confined in a slit pore. Labik and Smith reported NVT-ensemble Monte Carlo simulation results

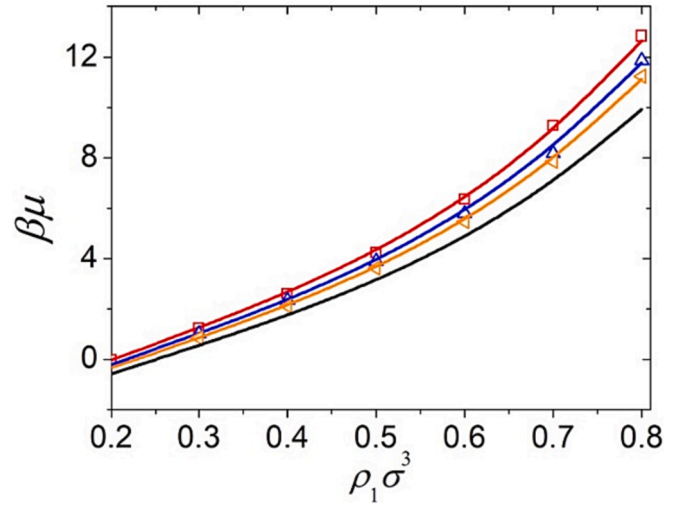


Fig. 2. Chemical potential of a hard sphere fluid confined in a slit pore as a function of fluid density from morphological thermodynamics, i.e., Eq. (12) (continuous line) and NVT-ensemble Monte-Carlo simulations (symbols, see Appendix B for the details about simulation method and computation conditions). 1) $L^* = 3.5$ (red); 2) $L^* = 5.0$ (blue); 3) $L^* = 7.5$ (yellow); 4) $L^* \rightarrow \infty$ (black).

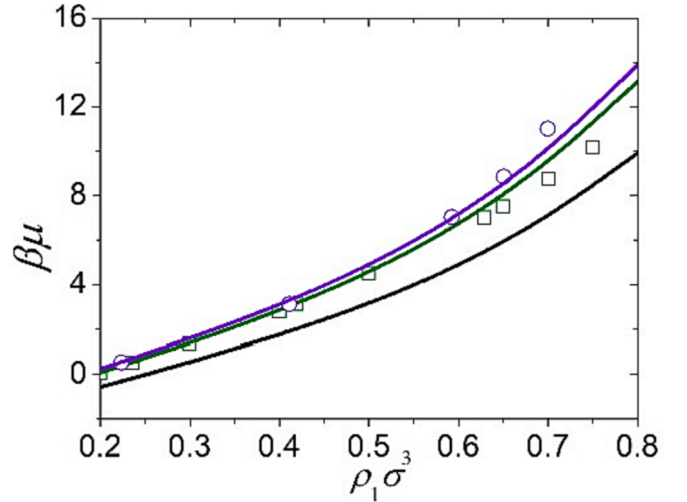


Fig. 3. Chemical potential of a hard sphere fluid confined in a narrow slit pore as a function of fluid density from morphological thermodynamics, i.e., eq. (12) (continuous line) and NVT-ensemble Monte-Carlo simulations (symbols, see Appendix B for the details about simulation method and computation conditions). 1) $L^* = 2.5$ (purple); 2) $L^* = 3.0$ (green); 3) $L^* \rightarrow \infty$ (black).

for hard spheres in a hard slit pore [25] and our simulation results are in good agreement with theirs. Smith and coworkers [26] and Alexandre et al [27] have used integral equations to study a hard sphere fluid in a slit pore. Many investigations on a variety of fluids confined in a slit pore have been made with the help of density functional theory (DFT) and many of them aim at determining the fluid distribution inside the pore (see e.g., [28], an exhaustive review is beyond the scope of the present article). The theoretical approaches based on DFT or integral equations requires first determining the one- and two-body distribution functions. Our approach in this work focuses only on the thermodynamic properties, which requires only the equation of state of the considered fluid in the bulk phase and the surface tension for the considered interface. When SPT is used for these properties, we obtain a totally analytical result for the adsorption isotherms of a hard sphere fluid confined in a slit pore.

3.2. A hard sphere fluid confined in an ordered or a disordered hard sphere matrix

The porous matrix model with quenched matrix particles proposed by Madden and Glandt [29] accounts for more characteristics of porous media than the simple slit pore model, e.g., pore connectivity, curved pore surface, variation of pore size inside a porous material. Fig. 4 illustrates three types of porous matrices: i) ordered hard sphere matrix with matrix particles fixed on a lattice; ii) disordered hard sphere matrix with matrix particles quenched from an equilibrium configuration of a fluid [29]; iii) overlapping hard sphere matrix with matrix particles distributed totally randomly in space. By construction, the morphological thermodynamics cannot distinguish the matrices of types i and ii.

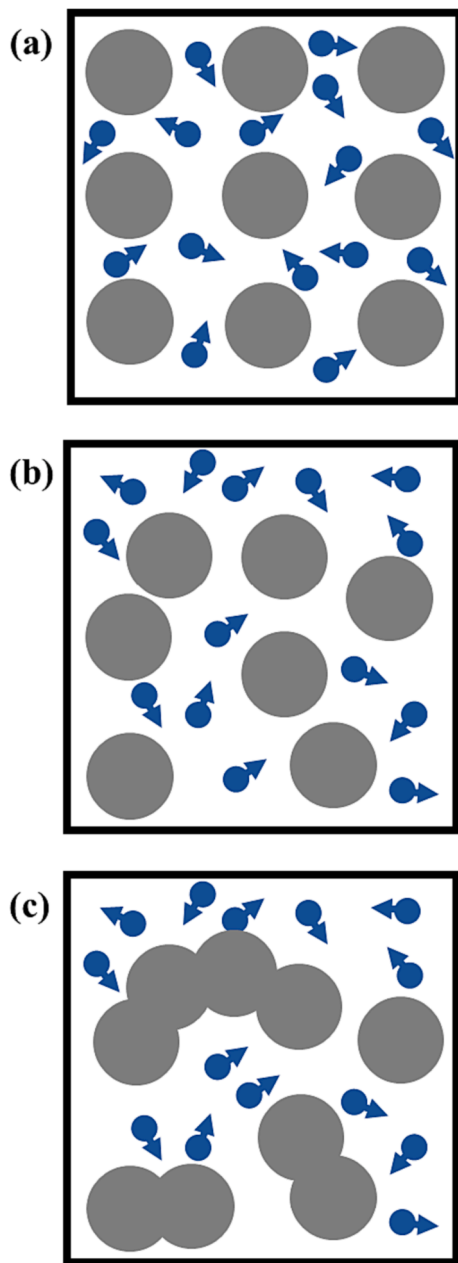


Fig. 4. Schematic presentation of a fluid of hard spheres (blue spheres) confined in different porous matrices composed of quenched matrix particles (grey). a) ordered porous matrix with hard sphere matrix particles fixed on a simple cubic lattice; b) hard sphere matrix quenched from an equilibrium liquid configuration; c) overlapping hard sphere matrix with matrix particles distributed totally randomly in space.

When the dividing surface is chosen as the surface of HS matrix particles, the fluid-matrix interface area of type i or ii matrices can be calculated easily and we have,

$$A = \pi\sigma_0^2 N_0 \quad (13)$$

where N_0 and σ_0 are respectively the number and diameter of the matrix particle.

The fundamental assumption of the morphological thermodynamics for treating the type i and type ii matrices is to describe the adsorption as the sum of adsorption around each matrix particle. SPT gives the following result for the adsorption around the surface of one matrix particle,

$$\begin{aligned} \pi\sigma_0^2\Gamma_s^{\text{SPT}} &= -\pi\sigma^2 \left(\frac{\partial\gamma^{\text{SPT}}}{\partial\mu^{\text{SPT}}} \right)_{T,\sigma_0} = -\pi\sigma^2 \left(\frac{\partial\gamma^{\text{SPT}}}{\partial\eta^b} \right)_{T,\sigma_0} / \left(\frac{\partial\mu^{\text{SPT}}}{\partial\eta^b} \right)_{T,\sigma_0} \\ &= -\frac{3\eta^b(1-\eta^b)}{1+2\eta^b} \left[\tau^2 + \frac{\tau(1-\eta^b)}{1+2\eta^b} + \frac{(1-\eta^b)^2}{3(1+2\eta^b)} \right] \end{aligned} \quad (14)$$

where $\tau = \sigma_0/\sigma$ is the size ratio between the matrix and fluid particles (σ_0 : matrix particle diameter). Besides the contribution given by Eq. (14), there is also an additional contribution to the adsorption given by,

$$\pi\sigma_0^2\Gamma_0 = \frac{(\phi_0^{\text{HS}} - 1)\rho^b V}{N_0} \quad (15)$$

where V is the volume of the matrix sample and ϕ_0^{HS} the geometric porosity for a hard sphere matrix,

$$\phi_0^{\text{HS}} = 1 - \frac{\pi\sigma_0^3 N_0}{6V} = 1 - \eta_0\tau^3 \quad (16)$$

with $\eta_0 = \pi\sigma^3 N_0 V^{-1} 6^{-1}$. Now, the relation between the packing fraction of the confined fluid and that of the bulk fluid with the same chemical potential is given by,

$$\eta_1 = \phi_0^{\text{HS}} \eta^b - \frac{3\eta_0 \eta^b (1-\eta^b)}{(1+2\eta^b)} \left[\tau^2 + \frac{\tau(1-\eta^b)}{1+2\eta^b} + \frac{(1-\eta^b)^2}{3(1+2\eta^b)} \right] \quad (17)$$

Unlike the case of a slit pore, it is not possible to solve Eq. (17) for obtaining an analytical expression of η^b in terms of η_1 like Eq. (11). Nevertheless, it is still quite easy to obtain the adsorption isotherm of the confined fluid with the following procedure. With a given ρ^b , one obtains a value of chemical potential, μ , and the fluid density of the confined fluid having the same chemical potential is given by Eq. (17), thus the relation between μ and η_1 is found. When the size of the fluid HS shrinks to zero, i.e., $\sigma = 0$, Eq. (17) becomes $\rho_1 = \phi_0^{\text{HS}} \rho^b$ and this allows for obtaining the exact result for an ideal gas confined in a HS matrix, i.e., $\beta\mu = \ln(\Lambda^3 \rho_1 / \phi_0^{\text{HS}})$. So, without the additional contribution to the adsorption given in Eq. (15), it is impossible to recover the exact ideal gas results in the limit of point particles. A more detailed discussion about this point is presented in Appendix A.

The results for a HS fluid confined in two ordered HS matrices with different matrix particle sizes and matrix densities are presented in Fig. 5. The analytical approach by combining morphological thermodynamics and SPT gives excellent results for the chemical potential, as evidenced by the comparison with the results of the Monte-Carlo simulations we performed. It is to note that we define the density of a fluid confined in a porous matrix with respect to the sample volume which contains fluid and matrix particles. Due to this definition, the range of fluid densities considered for fluids confined in porous matrices appears smaller than that considered for a fluid confined in a slit pore. For example, in Figs. 2 and 3 the considered fluid density goes up to 0.8 while the fluid density considered in Fig. 5 goes only to 0.6. In fact, to make a more plausible comparison between the fluid density in a porous matrix and that in a slit pore, we should take into account the porosity of

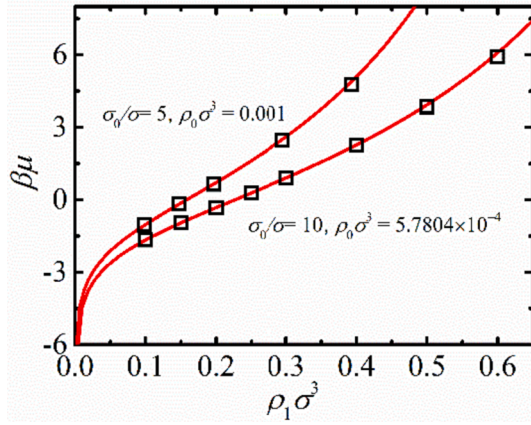


Fig. 5. Chemical potential of a hard sphere fluid confined in an ordered porous matrix, with hard sphere matrix particles fixed on a simple cubic lattice, as a function of fluid density. Matrix to fluid particle size ratio: $\sigma_0/\sigma = 5, 10$; Matrix density: $\rho_0\sigma^3 = 0.001, 5.7804 \times 10^{-4}$; Red lines: Morphological thermodynamics combined with SPT; Black squares: NVT-ensemble Monte-Carlo simulation (see Appendix B for the details about simulation method and computation conditions).

the porous matrix. For the matrix with $\sigma_0/\sigma = 10$ and $\rho_0\sigma^3 = 5.7804 \times 10^{-4}$ in Fig. 5, the porosity is given by $\phi_0 = 1 - \pi\rho_0\sigma_0^3/6 = 0.69734$. Dividing the fluid density defined with respect to the sample volume by the porosity give the fluid density defined with respect to the void volume. So, $\rho_1\sigma^3 = 0.6$ corresponds in fact to a fluid density defined with respect to void volume equal to $\rho_1\sigma^3/\phi_0 = 0.86$.

We consider next the effect of matrix disorder on the chemical potential of the confined fluid. The results for a HS fluid confined in a disordered HS matrix are presented in Fig. 6. By construction, the morphological thermodynamics does not take the effect of matrix disorder into account. However, our Monte-Carlo simulation results given in Fig. 6 are performed for disordered HS matrices (see Appendix B for simulation methods and computation conditions). The very good agreement between the results of the morphological thermodynamics and the simulation ones show that the effect of matrix disorder on the chemical potential is negligibly small. This conforms also to the same finding of our recent work [30]. In Fig. 6, the results of the morphological thermodynamics are also compared to those of SPT2b1 theory we proposed previously [16], which is an approach developed specifically for disordered porous matrices while the morphological thermodynamics is a general approach applicable for a larger variety of inhomogeneous fluids.

3.3. A hard sphere fluid confined in an overlapping hard sphere matrix

The application of morphological thermodynamics to this case follows the general procedure described above. So, we need first determine the porosity of the matrix for a point particle, ϕ_0 , which is required for determining ideal gas contribution to the chemical potential.

$$\begin{aligned} \phi_0^{\text{OHS}} &= \frac{1}{V} \int d\mathbf{r} \prod_{i=1}^{N_0} \int d\mathbf{q}_i e^{-\beta \sum_{j=1}^{N_0} u_{\text{fm}}(|\mathbf{r}-\mathbf{q}_j|)} = \frac{1}{V^{N_0}} \left(V - \frac{4\pi R_0^3}{3} \right)^{N_0} \\ &= \exp\left(-\frac{4\pi R_0^3 \rho_0}{3}\right) = \exp(-\eta_0 \tau^3) \end{aligned} \quad (18)$$

where \mathbf{r} is the position vector of the point particle and \mathbf{q}_i the position vector of the i -th matrix particle. The interaction between the point particle and a matrix particle is given by,

$$u_{\text{fm}}(|\mathbf{r}-\mathbf{q}_j|) = \begin{cases} \infty, & |\mathbf{r}-\mathbf{q}_j| < R_0 \\ 0, & |\mathbf{r}-\mathbf{q}_j| \geq R_0 \end{cases} \quad (19)$$

with $R_0 = \sigma_0/2$. The thermodynamic limit is taken, i. e., $\lim_{N_0 \rightarrow \infty, V \rightarrow \infty} N_0/V = \rho_0$, when going to the third equality of Eq. (18). The interface area is given by,

$$A^{\text{OHS}} = \frac{d(V - \phi_0^{\text{OHS}} V)}{dR_0} = V 4\pi R_0^2 \rho_0 \exp\left(-\frac{4\pi R_0^3 \rho_0}{3}\right) = V 4\pi R_0^2 \rho_0 \phi_0^{\text{OHS}} \quad (20)$$

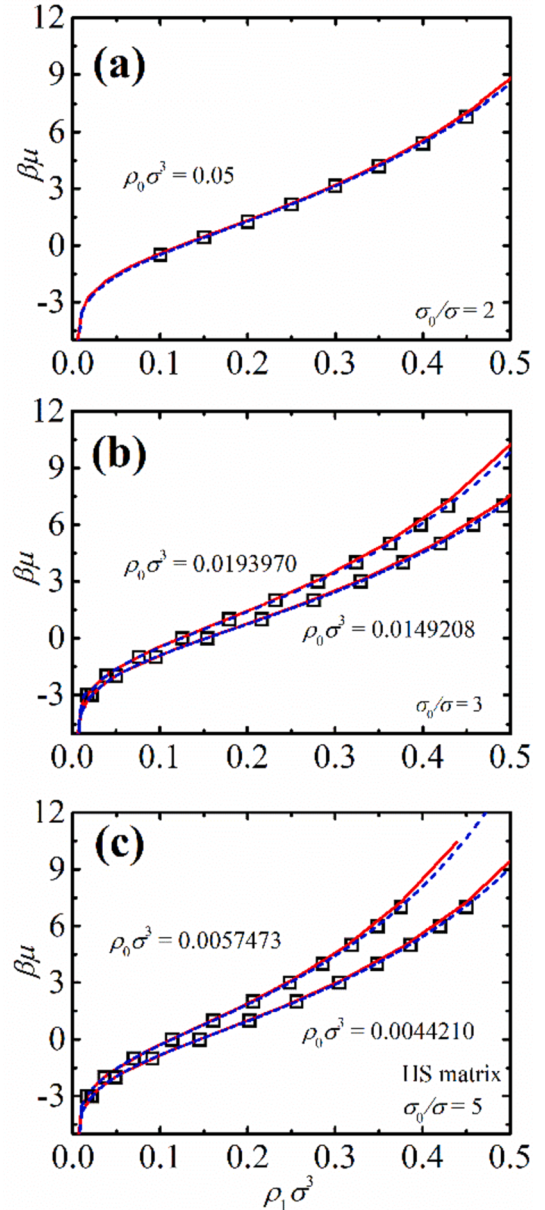


Fig. 6. Chemical potential of a hard sphere fluid confined in a disordered hard sphere matrix as a function of fluid density. a) Matrix to fluid particle size ratio: $\sigma_0/\sigma = 2$; Matrix density: $\rho_0\sigma^3 = 0.05$; b) Matrix to fluid particle size ratio: $\sigma_0/\sigma = 3$; Matrix density: $\rho_0\sigma^3 = 0.0149208, 0.019397$; c) Matrix to fluid particle size ratio: $\sigma_0/\sigma = 5$; Matrix density: $\rho_0\sigma^3 = 0.004421, 0.0057473$; Red lines: Morphological thermodynamics combined with SPT; Blue dashed lines: SPT2b1 theory [16]; Black squares: Monte-Carlo simulation (Results in (a) from our NVT-ensemble Monte-Carlo simulations with the details of simulation method and computation conditions given in Appendix B, those in (b) and (c) from the μ VVT-ensemble Monte-Carlo simulations given in Table III of [15]).

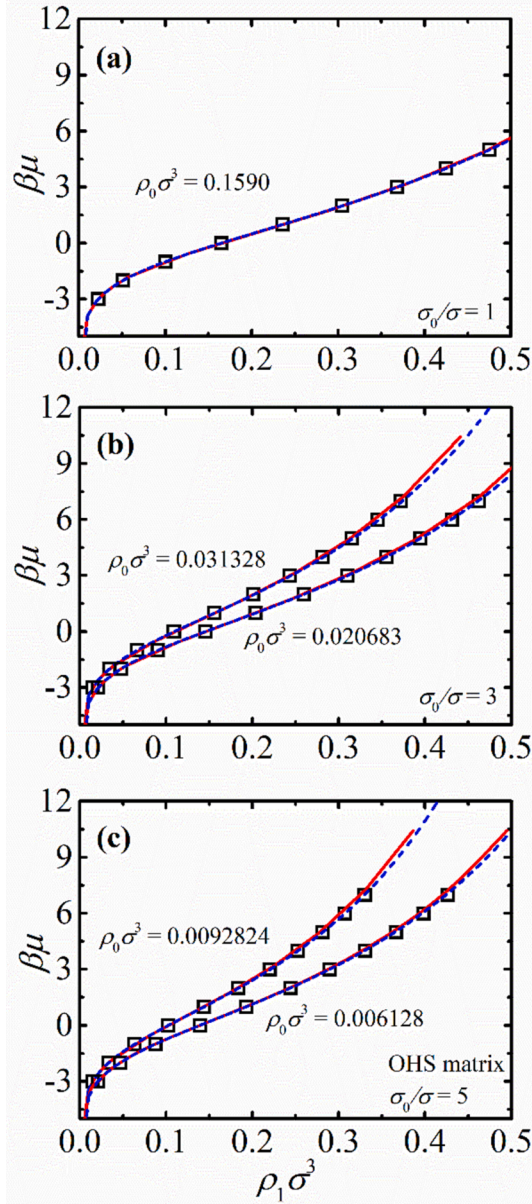


Fig. 7. Chemical potential of a hard sphere fluid confined in an overlapping hard sphere matrix as a function of fluid density. Red lines: Morphological thermodynamics combined with SPT; Blue dashed lines: SPT2b1 theory [16]; Black squares: Monte-Carlo simulation (Results in (a) from our NVT-ensemble Monte-Carlo simulations with the details of simulation method and computation conditions given in Appendix B, those in (b) and (c) from μ VT-ensemble Monte-Carlo simulations of [15]). a) Matrix to fluid particle size ratio: $\sigma_0/\sigma = 1$; Matrix density: $\rho_0\sigma^3 = 0.1590$ (the red line and the blue dashed lines nearly overlap each other); b) Matrix to fluid particle size ratio: $\sigma_0/\sigma = 3$; Matrix density: $\rho_0\sigma^3 = 0.020683, 0.031328$; c) Matrix to fluid particle size ratio: $\sigma_0/\sigma = 5$; Matrix density: $\rho_0\sigma^3 = 0.006128, 0.0092824$.

The integrated mean and Gauss curvatures are given respectively by,

$$\begin{aligned} C_M^{\text{OHS}} &= \frac{1}{2} \frac{dA}{dR_0} = V4\pi R_0 \rho_0 (1 - 2\pi R_0^3 \rho_0) \exp\left(-\frac{4\pi R_0^3 \rho_0}{3}\right) \\ &= V4\pi R_0 \rho_0 \left(1 - \frac{3}{2}\eta_0 \tau^3\right) \phi_0^{\text{OHS}} \end{aligned} \quad (21)$$

$$\begin{aligned} C_G^{\text{OHS}} &= \frac{1}{2} \frac{d^2A}{dR_0^2} = V4\pi \rho_0 (1 - 12\pi R_0^3 \rho_0 + 8\pi R_0^6 \rho_0^2) \exp\left(-\frac{4\pi R_0^3 \rho_0}{3}\right) \\ &= V4\pi \rho_0 \left(1 - 9\eta_0 \tau^3 + \frac{9}{2}\eta_0^2 \tau^6\right) \phi_0^{\text{OHS}} \end{aligned} \quad (22)$$

Finally, the morphological thermodynamics combined with SPT gives the following relation between the density of the confined fluid to that of the bulk fluid which has the same chemical potential,

$$\begin{aligned} \eta_1 &= \phi_0^{\text{OHS}} \eta^b - \frac{3\eta_0 \eta^b (1 - \eta^b)}{(1 + 2\eta^b)} \phi_0^{\text{OHS}} \left[\tau^2 + \frac{\tau(1 - \eta^b)}{1 + 2\eta^b} \left(1 - \frac{3}{2}\eta_0 \tau^3\right) \right. \\ &\quad \left. + \frac{(1 - \eta^b)^2}{3(1 + 2\eta^b)} \left(1 - 9\eta_0 \tau^3 + \frac{9}{2}\eta_0^2 \tau^6\right) \right] \end{aligned} \quad (23)$$

The results for a HS fluid confined in an overlapping hard sphere matrix are presented in Fig. 7. The results given by morphological thermodynamics are again in excellent agreement with the simulation ones under all the conditions we have studied.

3.4. A hard sphere fluid confined in a hard sponge matrix

The last system we consider is a hard sphere fluid confined in a hard sponge model proposed by two of us (SLZ and WD) with Q. H. Liu [31]. Fig. 8 gives a schematic presentation of this model. In this case, the interaction potential between a fluid particle and the matrix is a non-additive n-body one given by,

$$v_{\text{fm}}(\mathbf{r}; \mathbf{q}_1, \mathbf{q}_2, \dots, \mathbf{q}_{N_0}) = -k_B T \ln \left[1 - e^{-\beta \sum_{j=1}^{N_0} u_{\text{fm}}(|\mathbf{r} - \mathbf{q}_j|)} \right] \quad (24)$$

where $u_{\text{fm}}(|\mathbf{r} - \mathbf{q}_j|)$ is given by Eq. (19) and now σ_0 is the diameter of a spherical cavity in the sponge matrix. Although this fluid-matrix interaction potential is non-additive, it is still possible to obtain an analytical result for the porosity, i.e.,

$$\begin{aligned} \phi_0^{\text{HSG}} &= \frac{1}{V V^{N_0}} \int d\mathbf{r} \prod_{i=1}^{N_0} \int d\mathbf{q}_i e^{-\beta v_{\text{fm}}(\mathbf{r}; \mathbf{q}_1, \mathbf{q}_2, \dots, \mathbf{q}_{N_0})} \\ &= \frac{1}{V V^{N_0}} \int d\mathbf{r} \prod_{i=1}^{N_0} \int d\mathbf{q}_i \left[1 - e^{-\beta \sum_{j=1}^{N_0} u_{\text{fm}}(|\mathbf{r} - \mathbf{q}_j|)} \right] \\ &= 1 - \frac{1}{V^{N_0}} \left(V - \frac{\pi \sigma_0^3}{6} \right)^{N_0} = 1 - \exp\left(-\frac{\pi \sigma_0^3 \rho_0}{6}\right) = 1 - \phi_0^{\text{OHS}} \end{aligned} \quad (25)$$

The thermodynamic limit is taken, i.e., $\lim_{N_0 \rightarrow \infty, V \rightarrow \infty} N_0/V = \rho_0$, when going to the fourth equality of eq.(25). It is not difficult to see that if the cavity

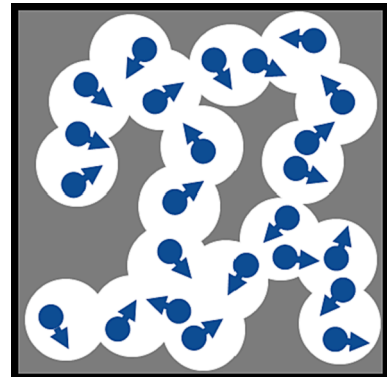


Fig. 8. Schematic presentation of a fluid of hard spheres (blue spheres) confined in a hard sponge matrix (grey).

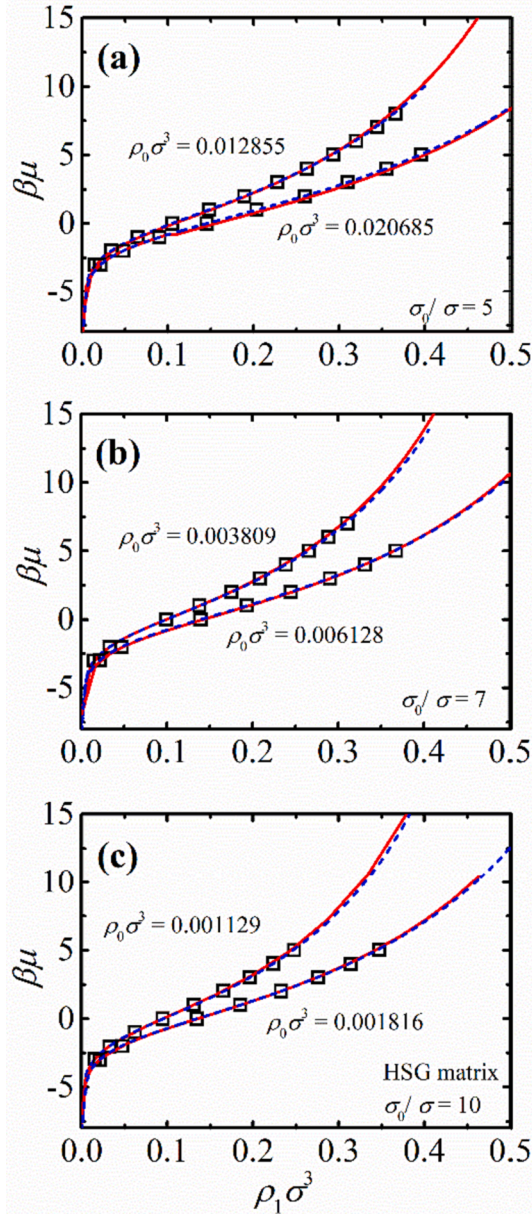


Fig. 9. Chemical potential of a hard sphere fluid confined in a hard sponge matrix as a function of fluid density. a) Cavity to fluid particle size ratio: $\sigma_0/\sigma = 5$; Cavity center density: $\rho_0\sigma^3 = 0.020685, 0.012855$; b) Cavity to fluid particle size ratio: $\sigma_0/\sigma = 7$; Cavity center density: $\rho_0\sigma^3 = 0.006128, 0.003809$; c) Cavity to fluid particle size ratio: $\sigma_0/\sigma = 10$; Cavity center density: $\rho_0\sigma^3 = 0.001816, 0.001129$; Red lines: Morphological thermodynamics combined with SPT; Blue dashed lines: SPT2b1 theory [16]; Black squares: μ VT-ensemble Monte-Carlo simulations (results from Fig. 4 of [16]).

diameter is the same as that of the matrix particle in an OHS matrix and their number densities are also equal, the following relations hold between the interface area, integrated mean and Gauss curvatures of the hard sponge matrix and those of the OHS matrix,

$$A^{\text{HSG}} = A^{\text{OHS}} \quad (26)$$

$$C_M^{\text{HSG}} = -C_M^{\text{OHS}} \quad (27)$$

$$C_G^{\text{HSG}} = C_G^{\text{OHS}} \quad (28)$$

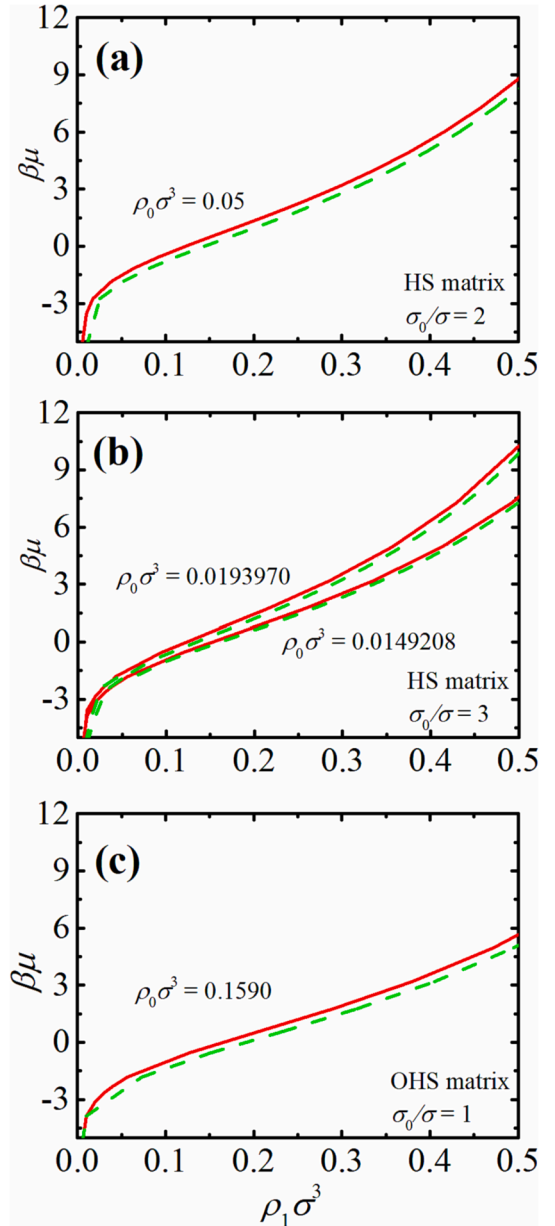


Fig. 10. Comparison of the results for the chemical potential of a confined fluid given by the full morphological thermodynamics (full orange lines) and by its simplified version without the contribution of curvature terms (dashed green lines). a) a HS fluid in a HS matrix with size ratio $\sigma_0/\sigma = 2$ and matrix density $\rho_0\sigma^3 = 0.05$; b) a HS fluid in a HS matrix with size ratio $\sigma_0/\sigma = 3$ and matrix density $\rho_0\sigma^3 = 0.0149208, 0.019397$; c) a HS fluid in an overlapping HS matrix with size ratio $\sigma_0/\sigma = 1$ and matrix density $\rho_0\sigma^3 = 0.1590$.

The relation given in Eq. (27) reflects the simple fact that the confined fluid is adsorbed on a convex surface in a OHS matrix but on a concave surface in a hard sponge matrix.

In Fig. 9, the results of the morphological thermodynamics for a HS fluid in a hard sponge matrix are presented along with simulation results under different conditions. The accuracy of our approach based on the morphological thermodynamics is again remarkable.

3.5. Contribution of surface curvatures

The comparison of the respective results for OHS and hard sponge matrices indicates that the contribution of the surface curvature terms to the adsorption isotherm can be quite small. More detailed analyses show

that when the matrix particle is three times larger than the fluid particle, the contribution of the surface curvatures is negligible. Fig. 10 shows that even for the size ratio ($\tau = \sigma_0/\sigma$) equal to 1, 2 or 3, the contribution of the surface curvatures is quite moderate. Bryk et al have studied the adsorption of hard spheres confined between two uniaxial cylinders by using DFT. They compared the results for such a confined fluid with those for a HS fluid confined in a slit pore of two flat walls and found that the surface curvature effect is quite small [32]. Our results presented in Fig. 10 are consistent with their finding. To the best of our knowledge, there exist no experimental technique for measuring the interface curvatures of any porous materials. So, our finding here provides a simplified procedure to interpret the experimental results for adsorption isotherms by neglecting the contribution of surface curvature terms.

4. Conclusion

In the present work, we propose a general approach based on the morphological thermodynamics for determining the chemical potential of a fluid confined in a large variety of porous media, from a simple slit pore to a random hard sponge matrix. Our approach requires an equation of state of the considered fluid in a bulk phase and the surface tension of the fluid on a wall with a much simpler morphology than the complex porous medium under consideration. For the hard sphere fluid confined in the various hard porous media considered in this work, scaled particle theory gives both the equation of state of the bulk fluid and the surface tension for a HS fluid on a hard-sphere wall. These are enough for constructing a totally analytical approach for all porous media considered in the present work. The comparison with simulation results show that the overall accuracy of our approach is excellent. Moderate discrepancies are found only for very narrow slit pores ($L \leq 3\sigma$) and at high fluid densities.

Although previous investigations have shown that non-Hadwiger terms (high-order curvature terms not included in morphological

thermodynamics) do not vanish rigorously [9–12], their contributions are usually smaller by one order of magnitude. In the present work, we find that even the integrated mean and Gauss curvature terms have a negligible contribution to the chemical potential of the confined fluid when the surface curvature is not too large. So, even the contribution of the integrated mean and Gauss curvatures can be neglected in many cases. This simplify significantly the treatment of the experimental results for the adsorption isotherms in practice since the experimental technique is currently lacking for measuring the interface curvatures inside a porous material. Thus, it is in principle possible to elaborate an experimental method for determining the surface tension for the interface between a fluid and the pore wall inside a porous material, with the help of its adsorption isotherms.

Declaration of competing interest

The authors declare that they have no known competing financial interests or personal relationships that could have appeared to influence the work reported in this paper.

Data availability

Data will be made available on request.

Acknowledgement

This work is supported by the National Natural Science Foundation of China (Nos. 22008063 and 22178072), the Guangxi Science and Technology Base and Talent Special Project (No. AD21220017). CZQ thanks the National Natural Science Foundation of China for the financial support (project No. 22008063). HRJ is grateful for the Eiffel scholarship of the French government and the CSC scholarship of the Chinese government.

Appendix A. An ideal gas confined in a hard sphere matrix

In this appendix, we show how surface thermodynamics can be applied for an ideal gas adsorbed in a hard sphere matrix and how the surface tension can be defined in this case. As in the main text, we consider a grand canonic ensemble. The fluid-matrix interaction is given by,

$$\mathcal{V} = \sum_{i=1}^N \sum_{j=1}^{N_0} u_{fm}(|\mathbf{r}_i - \mathbf{q}_j|) \quad (\text{A1})$$

where \mathbf{r}_i is the position vector of i th fluid particle and \mathbf{q}_j the position vector of j th matrix particle. The interaction potential between a fluid particle and a matrix particle is given by,

$$u_{fm}(|\mathbf{r}_i - \mathbf{q}_j|) = \begin{cases} \infty, & |\mathbf{r}_i - \mathbf{q}_j| < R_0 \\ 0, & |\mathbf{r}_i - \mathbf{q}_j| \geq R_0 \end{cases} \quad (\text{A2})$$

The partition is given by,

$$\Xi = \sum_{N=0}^{\infty} \frac{e^{\beta\mu N}}{\Lambda^{3N} N!} \int_V \prod_{i=1}^N d\mathbf{r}_i e^{-\beta \mathcal{V}} = \sum_{N=0}^{\infty} \frac{e^{\beta\mu N}}{\Lambda^{3N} N!} \left(V - \frac{4\pi R_0^3 N_0}{3} \right)^N = \exp \left[\frac{e^{\beta\mu}}{\Lambda^3} \left(V - \frac{4\pi R_0^3 N_0}{3} \right) \right] \quad (\text{A3})$$

One obtains straightforwardly following result for the grand potential,

$$\Omega = -k_B T \ln \Xi = -k_B T \frac{e^{\beta\mu}}{\Lambda^3} V \phi_0^{\text{HS}} \quad (\text{A4})$$

Eq. (A4) shows that the grand partition function does not depend on the configuration of the porous matrices. So, the disorder of the matrix configurations does not have any influence on the thermodynamics of this system. Moreover, the grand potential does not depend on the surface area of the matrix particle. Thus, the immediate consequence of this is that the differential surface tension is zero, i.e.,

$$\gamma = \left(\frac{\partial \Omega}{\partial A} \right)_{T, V, \mu, \rho_0, R_0} = 0 \quad (\text{A5})$$

At the first glance, this indicates that surface thermodynamics does not apply for such a system. However, it is also straightforward to show that the adsorption in this hard sphere matrix is not zero. The number of the confined fluid inside the matrix is given by,

$$N^{\text{cf}} = - \left(\frac{\partial \Omega}{\partial \mu} \right)_{T, V, A, \rho_0, R_0} = \frac{e^{\beta \mu}}{\Lambda^3} V \phi_0^{\text{HS}} \quad (\text{A6})$$

However, the number of a bulk ideal gas occupying the same volume and having the same temperature and the same chemical potential is given by,

$$N^{\text{bulk}} = \frac{e^{\beta \mu}}{\Lambda^3} V \quad (\text{A7})$$

Eqs. (A6) and (A7) lead immediately to the following nonzero adsorption,

$$\Gamma = \frac{N^{\text{cf}} - N^{\text{bulk}}}{A} = \frac{e^{\beta \mu}}{\Lambda^3} \frac{V}{A} (\phi_0^{\text{HS}} - 1) \quad (\text{A8})$$

The well-known Gibbs adsorption equation implies that a nonzero adsorption should lead to a nonzero surface tension. So, this result seems to be in contradiction with that of Eq. (A5) which shows the surface tension is zero.

Now, we will show that there is in fact no contradiction. It is recently revealed that two surface tensions can arise, one is the differential surface tension and the other is the integral surface tension [18,19]. Moreover, it is the integral surface tension which satisfies a generalized Gibbs adsorption equation [18]. The integral surface tension includes a contribution from the differential surface tension and another contribution from the disjoining pressure. We calculate now the disjoining pressure and show it is indeed nonzero for the system considered here. The pressures of the confined and bulk fluids are given respectively by,

$$p = - \left(\frac{\partial \Omega}{\partial V} \right)_{T, A, \mu, \rho_0, R_0} = k_B T \frac{e^{\beta \mu}}{\Lambda^3} \phi_0^{\text{HS}} \quad (\text{A9})$$

$$p^{\text{bulk}} = - \left(\frac{\partial \Omega^{\text{bulk}}}{\partial V} \right)_{T, \mu,} = k_B T \frac{e^{\beta \mu}}{\Lambda^3} \quad (\text{A10})$$

Then, one obtains the following result for the disjoining pressure,

$$\Pi = p - p^{\text{bulk}} = k_B T \frac{e^{\beta \mu}}{\Lambda^3} (\phi_0^{\text{HS}} - 1) \quad (\text{A11})$$

Disjoining pressure was discovered by Derjaguin in 1930's for a fluid confined between two closely approached flat solid surfaces [23,24]. To the best of our knowledge, nonzero disjoining pressure has never been found for a fluid confined in a fluid confined in a porous matrix. The integral surface tension is given by,

$$\hat{\gamma} = \gamma - \Pi \frac{V}{A} = -k_B T \frac{e^{\beta \mu}}{\Lambda^3} (\phi_0^{\text{HS}} - 1) \frac{V}{A} \quad (\text{A12})$$

One readily check that this integral surface tension and the adsorption given in Eq. (8) satisfies the following generalized Gibbs adsorption equation [18,19], i.e.,

$$\left(\frac{\partial \hat{\gamma}}{\partial \mu} \right)_{T, \hat{\gamma}} = -\Gamma \quad (\text{A13})$$

where $\hat{\gamma} = V/A$

Finally, we show that accounting adequately for the integral surface tension and the related adsorption allows for introducing properly the porosity, ϕ_0 , into the adsorption isotherms, i.e., the chemical potential as a function of the density of the confined fluid. From Eq. (A7), one has the following equation of state for the bulk ideal gas,

$$\beta \mu^{\text{bulk}} = \ln(\Lambda^3 \rho^{\text{bulk}}) \quad (\text{A14})$$

From Eqs. (A6)–(A8), we obtain,

$$\rho^{\text{bulk}} = \rho^{\text{cf}} - \Gamma \frac{A}{V} = \rho^{\text{cf}} - \rho^{\text{cf}} \frac{\phi_0^{\text{HS}} - 1}{\phi_0^{\text{HS}}} = \frac{\rho^{\text{cf}}}{\phi_0^{\text{HS}}} \quad (\text{A15})$$

where $\rho^{\text{bulk}} = N^{\text{bulk}} V^{-1}$, $\rho^{\text{cf}} = N^{\text{cf}} V^{-1}$. Substituting Eq. (A15) into Eq. (A14), we obtain,

$$\beta \mu^{\text{bulk}} = \ln \left(\frac{\Lambda^3 \rho^{\text{cf}}}{\phi_0^{\text{HS}}} \right) = \beta \mu^{\text{cf}} \quad (\text{A16})$$

When going to the last equality of Eq. (A16), Eq. (A6) is used. This achieves the proof that the matrix porosity enters into the isotherm of adsorption, i.e., the relation between the chemical potential and the density of the confined fluid, through the adsorption due to the disjoining pressure.

Appendix B. Simulation method and computational conditions

In the main text, accompanying the presentation of the results given by morphological thermodynamics, Monte-Carlo simulation results are also presented to assess the accuracy of theoretical approach in each case. Except those results with their references being indicated, all the other ones are obtained from our own simulations. In this appendix, we summarize the simulation methods and the computation conditions for each porous medium.

1. Fluid in a slit pore

The Monte-Carlo simulation results presented in Figs. 2 and 3 are obtained by our own simulation in a NVT-ensemble. The chemical potential is calculated by using the test particle method based on Widom's potential distribution theorem [33]. The two pore walls are respectively placed at $z = \pm L/2$. The pore wall has a square shape of the size $10\sigma \times 10\sigma$. The periodic boundary condition is used in the two directions parallel to the pore walls. For each simulation run, 2×10^5 Monte-Carlo cycles are first performed to prepare the system to equilibrium, then 10^6 MC cycles are performed to calculate the chemical potential.

2. Fluid in various porous matrices

For the ordered porous matrix (results shown in Fig. 5), we studied only the case with matrix particles placed on a simple cubic lattice. A single matrix particle is placed at the center of the cubic simulation box. The periodic boundary condition is applied in three directions to generate a simple cubic lattice. The simulation box has respectively the size of $20\sigma \times 20\sigma \times 20\sigma$ and $36\sigma \times 36\sigma \times 36\sigma$ for the cases of $\sigma_0 = 5\sigma$ and $\sigma_0 = 10\sigma$.

For the disordered HS matrix (results shown in Fig. 6), a matrix sample is first generated with an NVT-ensemble Monte-Carlo simulation for 50 hard spheres of diameter σ_0 in a simulation box of the size $10\sigma \times 10\sigma \times 10\sigma$. Then, fluid particles are introduced into the HS matrix and NVT-ensemble Monte-Carlo simulations are performed for the confined fluid. The average over matrix configurations is realized with about 10–20 different matrix samples.

For the overlapping hard sphere matrix (results shown in Fig. 7a), 159 matrix particles with the same diameter as the fluid particle, i.e. $\sigma_0 = \sigma$, are placed totally randomly in the simulation box of the size, $10\sigma \times 10\sigma \times 10\sigma$. The average over matrix configurations is realized with 10 different matrix samples.

As for the slit pore, each simulation for a given matrix sample includes about 2×10^5 Monte-Carlo cycles for preparing the system to equilibrium and 10^6 production cycles for determining the chemical potential. The simulation code can be found on GitHub (<https://github.com/qiaochongzhi/MC-for-ConfinedFluid>).

References

- [1] P.M. König, R. Roth, K.R. Mecke, Morphological Thermodynamics of Fluids: Shape Dependence of Free Energies, *Physical Review Letters* 93 (16) (2004), 160601.
- [2] K. Mecke, C.H. Arns, Fluids in Porous Media: A Morphometric Approach, *Journal of Physics: Condensed Matter* 17 (9) (2005) S503–S534.
- [3] R. Roth, Y. Harano, M. Kinoshita, Morphometric Approach to the Solvation Free Energy of Complex Molecules, *Physical Review Letters* 97 (7) (2006), 078101.
- [4] M. Oettel, H. Hansen-Goos, P. Bryk, R. Roth, Depletion Interaction of Two Spheres—Full Density Functional Theory vs. Morphometric Results. *EPL Europhysics Lett.* 85 (3) (2009) 36003.
- [5] R. Kodama, R. Roth, Y. Harano, M. Kinoshita, Morphometric approach to thermodynamic quantities of solvation of complex molecules: Extension to multicomponent solvent, *The Journal of Chemical Physics* 135 (2011), 045103.
- [6] Z. Jin, J. Kim, J. Wu, Shape Effect on Nanoparticle Solvation: A Comparison of Morphometric Thermodynamics and Microscopic Theories, *Langmuir* 28 (17) (2012) 6997–7006.
- [7] M.E. Evans, R. Roth, Solvation of a sponge-like geometry, *Pure and Applied Chemistry* 86 (2014) 173.
- [8] A. Reindl, M. Bier, S. Dietrich, Implications of Interface Conventions for Morphometric Thermodynamics, *Physical Review E* 91 (2) (2015), 022406.
- [9] B.B. Laird, A. Hunter, R.L. Davidchack, Interfacial Free Energy of a Hard-Sphere Fluid in Contact with Curved Hard Surfaces, *Physical Review E* 86 (6) (2012) 060602(R).
- [10] E.M. Blokhuis, Existence of a Bending Rigidity for a Hard-Sphere Liquid near a Curved Hard Wall: Validity of the Hadwiger Theorem, *Physical Review E* 87 (2) (2013), 022401.
- [11] I. Urrutia, Bending Rigidity and Higher-Order Curvature Terms for the Hard-Sphere Fluid near a Curved Wall, *Physical Review E* 89 (3) (2014), 032122.
- [12] H. Hansen-Goos, Communication: Non-Hadwiger Terms in Morphological Thermodynamics of Fluids, *The Journal of Chemical Physics* 141 (17) (2014), 171101.
- [13] M. Holovko, W. Dong, A Highly Accurate and Analytic Equation of State for a Hard Sphere Fluid in Random Porous Media, *The Journal of Physical Chemistry. B* 113 (18) (2009) 6360–6365.
- [14] W. Chen, W. Dong, M. Holovko, X.S. Chen, Comment on “A highly accurate and analytic equation of state for a hard sphere fluid in random porous media”, *The Journal of Physical Chemistry. B* 114 (2010) 1225.
- [15] T. Patsahan, M. Holovko, W. Dong, Fluids in Porous Media. III. Scaled Particle Theory, *The Journal of Chemical Physics* 134 (7) (2011), 074503.
- [16] M. Holovko, T. Patsahan, W. Dong, Fluids in Random Porous Media: Scaled Particle Theory, *Pure and Applied Chemistry* 85 (1) (2013) 115–133.
- [17] W. Chen, S.L. Zhao, M. Holovko, X.S. Chen, W. Dong, Scaled particle theory for multicomponent hard sphere fluids confined in random porous media, *The Journal of Physical Chemistry. B* 120 (2016) 5491.
- [18] W. Dong, Thermodynamics of interface extended to nanoscales by introducing integral and differential surface tensions, *PNAS* 118 (2021), e2019873118.
- [19] W. Dong, Nanoscale thermodynamics needs the concept of a disjoining chemical potential, *Nature Communications* 2023 (1824) 14.
- [20] H. Reiss, H.L. Frisch, J.L. Lebowitz, Statistical mechanics of rigid spheres, *The Journal of Chemical Physics* 31 (1959) 369.
- [21] W. Dong, X.S. Chen, Scaled particle theory for bulk and confined fluids: A review, *Science China - Physics Mechanics & Astronomy* 61 (2018), 070501.
- [22] C.Z. Qiao, S.L. Zhao, H.L. Liu, W. Dong, Augmented scaled particle theory, *The Journal of Physical Chemistry. B* 124 (2020) 1207.
- [23] B.V. Derjaguin, Y.I. Rabinovich, N.V. Churaev, Direct measurement of molecular forces, *Nature* 272 (1978) 313–318.
- [24] B.V. Derjaguin, N.V. Churaev, V.M. Muller, *Surface forces*, Springer Science+Business Media, LLC, 1987.
- [25] S. Labik, W.R. Smith, Computer simulation of the chemical potential and adsorption isotherm of hard spheres in a hard slit-like pore, *Molecular Physics* 88 (1996) 1411.
- [26] R. Pospisil, A. Malijevsky, P. Jech, W.R. Smith, Integral equation and computer simulation studies of hard spheres in a slit pore, *Molecular Physics* 78 (1993) 1461.
- [27] J. Alexandre, M. Lazasa-Cassou, L. Degève, Effect of pore geometry on a confined hard sphere fluid, *Molecular Physics* 88 (1996) 1317.
- [28] Y.X. Yu, J.Z. Wu, A modified fundamental measure theory for spherical particles in microchannels, *The Journal of Chemical Physics* 119 (2003) 2288.
- [29] W.G. Madden, E.D. Glandt, Distribution Functions for Fluids in Random Media, *Journal of Statistical Physics* 51 (3–4) (1988) 537–558.
- [30] C.Z. Qiao, S.L. Zhao, H.L. Liu, W. Dong, Connect the Thermodynamics of Bulk and Confined Fluids: Confinement-Adsorption Scaling, *Langmuir* 35 (10) (2019) 3840–3847.
- [31] S.L. Zhao, W. Dong, Q.H. Liu, Fluids in Porous Media. I. A Hard Sponge Model, *The Journal of Chemical Physics* 125 (2006), 244703.
- [32] P. Bryk, L. Lajtar, O. Pizio, Z. Sokolowska, S. Sokolowski, Adsorption of fluids in pores formed between two hard cylinders, *J. Colloid and Interface Sci.* 229 (2000) 526.
- [33] B. Widom, Some topics in the theory of fluids, *The Journal of Chemical Physics* 39 (1963) 2808.